SCIENCE CHINA
Earth Sciences

•ARTICLE•

https://doi.org/10.1007/s11430-023-1405-8

Tropical cyclone genesis over the western north Pacific in La Niña decay summers: Comparison between 2018 and 2021

Yunyun LIU[1,2] & Zhensong GONG[1*]

[1] *China Meteorological Administration Key Laboratory for Climate Prediction Studies, National Climate Centre, Beijing 100081, China;*
[2] *Collaborative Innovation Center on Forecast and Evaluation of Meteorological Disasters, Nanjing University of Information Science & Technology, Nanjing 210044, China*

Received November 7, 2023; revised July 17, 2024; accepted August 5, 2024; published online September 3, 2024

Abstract As the primary interannual signal of variability in the tropical ocean-atmosphere interaction, the El Niño-Southern Oscillation has a considerable impact on tropical cyclone (TC) activity over the western North Pacific (WNP). Both 2018 and 2021 were La Niña decay years, but TC activity over the WNP during the two summers (June–August) showed notable differences. In 2018, summer TC activity was unusually high with a total of 18 TCs, and the region of TC genesis was mainly in the central and eastern WNP. In contrast, only 9 TCs were generated in summer 2021, and the region of TC genesis was primarily in the western WNP. By comparing the characteristics of the large-scale environmental conditions over the regions of TC genesis, the thermal factors of the tropical oceans, and the activity of the Madden-Julian Oscillation (MJO), this study revealed the possible causes for the marked differences in TC genesis over the WNP during the two summers, which both had a similar background of La Niña decay. The Indian Ocean Basin Mode (IOBM) transitioned of a cold anomaly in the winter of 2017/2018 and persisted until summer 2018. At the same time, the Pacific Meridional Mode (PMM) maintained a positive phase, leading to eastward and northward displacement of the Western Pacific Subtropical High in summer, and eastward extension of the tropical monsoon trough, which presented conditions conducive to TC genesis over the Northwest Pacific. Moreover, the days when the MJO stagnated in phases 5 and 6 in the summer of 2018 increased by approximately 150% relative to climatological state, providing dynamic conditions favorable for TC formation. In 2021, the IOBM quickly turned to a warm anomaly in March and persisted until summer, whereas the PMM became a negative phase in January and remained so until summer. At the same time, the MJO stagnated in phases 2 and 3 for up to 47 days, with the center of convection located over the western Maritime Continent, producing conditions unconducive to TC genesis over the Northwest Pacific. Thus, despite being under a similar background of La Niña decaying year, the distinct evolutions of the IOBM, PMM, and MJO in spring and summer of 2018 and 2021 were the main causes of the notable differences in TC activity over the WNP during these two summers, and the anomalies in IOBM and MJO contributed more significantly than those of the PMM.

Keywords Tropical cyclone, La Niña events, Indian Ocean Basin Mode, Pacific Meridional Mode, Madden-Julian Oscillation, Western Pacific Subtropical High, Monsoon trough

Citation: Liu Y, Gong Z. 2024. Tropical cyclone genesis over the western north Pacific in La Niña decay summers: Comparison between 2018 and 2021. Science China Earth Sciences, 67, https://doi.org/10.1007/s11430-023-1405-8

1. Introduction

As one of the most destructive natural disasters, tropical cyclones (TCs) generated over the western North Pacific (WNP) account for approximately one-third of the TCs that occur globally each year (Chan, 2000). On average, seven to eight TCs make landfall on the southeastern and southern coasts of China annually, causing huge economic losses and numerous casualties (Zhang et al., 2011). Therefore, studies

* Corresponding author (email: gongzs@cma.gov.cn)

on TC activities over the WNP, accurate prediction of TC activities, and strengthening of TC defense capabilities are of great importance both for ensuring the safety of livelihoods and property, and for promoting sustainable regional socio-economic development.

Over the WNP, most TCs in summer form within a southeast-northwest extension of the monsoon trough, and their geneses are closely related to tropical disturbances (Briegel and Frank, 1997). The monsoon trough provides not only the large-scale environmental conditions favorable for TC genesis, such as low-level airflow convergence and cyclonic relative vorticity, upper-level airflow divergence, weak vertical wind shear, and abundant water vapor, but also the initial disturbances and dynamic conditions suitable for TC genesis (Chen and Huang, 2006). Furthermore, the evolution of the monsoon trough is closely related to the Western Pacific Subtropical High (WPSH). When the WPSH retreats from the South China Sea (SCS) to the vicinity of the Philippines, the monsoon trough correspondingly extends eastward, and the westerlies on its southern flank also extend eastward, creating conditions favorable for TC genesis over the southeastern WNP. Southward movement of the WPSH ridgeline also causes the location of TC genesis to become displaced further southeastward (Huangfu et al., 2018). Additionally, the WPSH can also affect TC track by guiding the airflow (Ho et al., 2004).

As one of the most important external forcing factors on the interannual timescale, the El Niño-Southern Oscillation (ENSO) cycle has a tremendous impact on TC activities over the WNP by affecting large-scale circulation systems such as the Walker circulation and the monsoon trough (Wang and Chan, 2002; Zhan et al., 2011; Han et al., 2016). In the summer of a developing El Niño, owing to the eastward development of the monsoon trough, TC is active over the southeastern WNP, and the frequency of TC genesis over the northwestern WNP is reduced, presenting a dipole distribution between the southeastern and northwestern regions of WNP TC genesis. In the summer of a developing La Niña, the frequency of TC genesis is broadly the converse. Thus, ENSO mainly affects the spatial distribution of TCs during its developing phase, rather than affecting the overall frequency of TC genesis (Wang and Chan, 2002). In the decaying phases of the eastern-Pacific El Niño, owing to the strong low-level anomalous anticyclone over the WNP, the number of TCs generated over the entire WNP is usually reduced (Zhan et al., 2011). In the past two decades, the central-Pacific El Niño phenomena occurred more frequently, and the relationship between the frequency of TC genesis and the year of El Niño decay was weakened (Wang et al., 2018), which reflects that the WPSH is often weaker in the summer of the year of central-Pacific El Niño decay than in the summer of eastern-Pacific El Niño decay (Stuecker et al., 2013; Zhang et al., 2015). However, in the summer of La Niña decay, the monsoon trough is weakened and the low-level absolute vorticity is reduced, inhibiting TC genesis near the SCS. Correspondingly, in terms of spatial distribution, TC genesis frequency occurs less often over both the western SCS and the southeastern WNP TC genesis regions, but it has a trend of increase over the central WNP (Liu et al., 2021). According to previous studies, such conditions cannot explain the notable differences in the frequency of TC genesis between 2018 and 2021 under similar ENSO phases and evolution backgrounds.

In addition to the ENSO cycle, other sea surface temperature anomaly (SSTA) modes, including the Indian Ocean Basin Mode (IOBM), Pacific Meridional Mode (PMM), and Tropical North Atlantic Mode, also have a substantial impact on TC activities over the WNP (Huangfu et al., 2019). The IOBM usually manifests as a response lagging one-two seasons behind the evolution of ENSO (Ashok et al., 2003). The positive phase of the IOBM stimulates eastward propagation of Kelvin waves, generating negative vorticity anomalies in the lower troposphere through Ekman pumping and diabatic cooling, which lead to a stronger and further southwestward extension of the WPSH that is unfavorable for TC genesis (Qian and Guan, 2019). The influence of the IOBM on the WPSH during spring and summer is greater than that of ENSO events (Liu and Gao, 2021). The PMM features a meridional seesaw of SSTAs accompanied by cross-equatorial surface winds (Chiang and Vimont, 2004). Typically, it influences TC activities by affecting the low-level circulation and monsoon trough anomalies over the WNP. It can serve as a predictor of TC genesis frequency independent of ENSO (Zhang et al., 2017b). Furthermore, several studies hypothesized possible linkages between SSTAs in the Tropical North Atlantic and WNP TC activities by adjusting the Walker circulation (Zhang et al., 2017a).

The Madden-Julian Oscillation (MJO), which is the most important mode of the tropical atmospheric circulation, is characterized as a large-scale tropical deep convection anomaly moving from the East Indian Ocean, across Indonesia, and into the West Pacific, disappearing near the dateline (Madden and Julian, 1971). However, even under similar SST backgrounds, MJO activity can exhibit completely different features, and the physical mechanisms that influence MJO activity have yet to be identified conclusively (Liu et al., 2021). Thus, the MJO is treated as an independent driving factor of the tropical circulation, summer precipitation, and WNP TC activities (Gong et al., 2022). When the MJO is in an active phase, it promotes the occurrence and development of convection, creating large-scale dynamic conditions favorable for TC genesis. As the MJO propagates eastward, cumulus convection continually develops and spreads, greatly influencing the heating configuration in the WNP, and regulating the generation and development of TCs (Gong et al., 2022). It also has a substantial impact on the

activity and paths of WNP TCs (Liu et al., 2021).

One of the main predictors for summer TC genesis is the SSTA in the central and eastern equatorial Pacific during the previous winter and spring. The winters of 2017/2018 and 2020/2021 were both La Niña years, with cold SSTAs in the central and eastern equatorial Pacific, which gradually turned to a neutral state in the spring of the following years. However, under similar ENSO evolution backgrounds, the frequency of TC genesis over the WNP presents obvious differences between the two La Niña decay summers. This raises questions regarding what caused the difference in TC activity over the WNP between the two years, and which factors other than the ENSO cycle should be considered when predicting TC genesis over the NWP. This study investigated and compared the large-scale environmental conditions, SSTA forcing, and MJO activities in the two years, and quantitatively evaluated the relative contributions to TC activity among those external forcing factors.

2. Data and methods

In this work, the meteorological elements associated with the large-scale environmental conditions for WNP TC activity, extracted from the National Centers for Environmental Prediction/National Center for Atmospheric Research reanalysis data with a spatial resolution of 2.5°×2.5°, included air temperature, relative and specific humidity, horizontal wind, vertical velocity, and sea level pressure (Kalnay et al., 1996). The global linear optimal interpolation SST data with spatial resolution of 1°×1° (i.e., the OISSTv2.1 data), starting from September1981, were provided by the National Oceanic and Atmospheric Administration (Huang et al., 2021). The information on TC occurrence frequency and genesis location was derived from the best typhoon track dataset provided by the Shanghai Typhoon Institute of the China Meteorological Administration (Ying et al., 2014). Anomalies of all variables were defined as deviations from the climatological mean of 1991–2020. The temporal range of the linear correlation in this work spanned 1991–2020, and according to the t-test standard, the correlation coefficient values corresponding to the 0.1, 0.05, and 0.01 significance levels were 0.30, 0.35, and 0.45, respectively.

The Niño3.4 index used here comprised the SSTA averaged over the area 5°S–5°N, 170°W–120°W, and the IOBM index comprised the SSTA averaged over the area 20°S–20°N, 40°E–110°E (Chambers et al., 1999). The PMM was the first mode obtained by singular value decomposition of the SST and surface wind field at 10-m height in the area 175°E–95°W, 21°S–32°N after removing seasonal trends and ENSO signals (Chiang, 2004). The specific calculation method can be found at the following website: https://psl.noaa.gov/data/timeseries/monthly/PMM. The real-time multivariate MJO index was selected as the monitoring and forecasting indicator for the MJO (Wheeler and Hendon, 2004). This index, which is composed of three variables (i.e., 850-hPa meridional wind, 200-hPa meridional wind, and outgoing longwave radiation (OLR)), reflects the large-scale circulation and deep convection coupling structure characteristics of the MJO. It is used widely in MJO monitoring and related studies, and the index data can be downloaded from the website of the Australian Bureau of Meteorology.

3. Comparison of TC activity between 2018 and 2021

The monthly frequency of TC genesis over the WNP during January–December and the monthly TC landfall frequency in China in June–October of both 2018 and 2021 are shown in Figure 1. In 2018, 29 TCs occurred over the WNP and 10 TCs made landfall over China, representing 4 and 3 more than the climatology, respectively. Among them, 18 TCs were generated in the summer, which was a number notably higher than the climatological mean value and the second highest since 1949. The frequency of TC genesis in each month from June to August was higher than the climatological mean value (Figure 1a). During summer 2018, eight TCs made landfall over China, which was a number more than twice the standard deviation of the climatology and the highest since 1949. The monthly frequency of TC landfall from June to August was also higher than the climatological

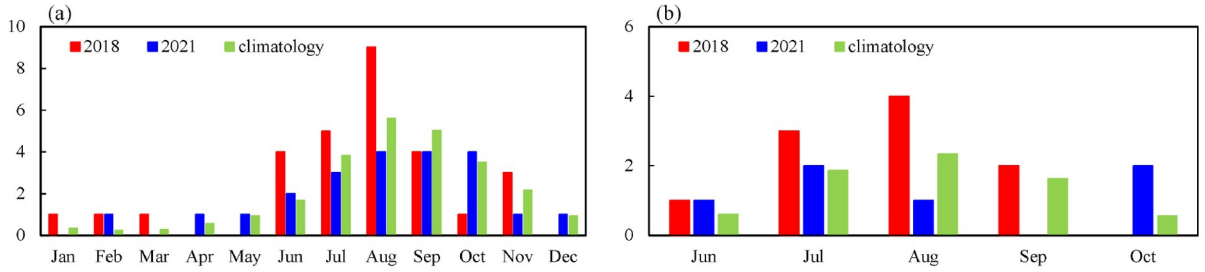

Figure 1 Monthly frequency of (a) TC genesis over the WNP and (b) TC landfall over China in 2018 (red bars) and 2021 (blue bars), together with the corresponding climatology (green bars).

value (Figure 1b). It is evident that TC activity in summer 2018 was characterized by continuously abnormal activity.

The situation in 2021 was different from that in 2018. Although 22 TCs occurred over the WNP, only 6 TCs made landfall over China, i.e., 3 and 1 less than the climatological mean values, respectively. Among them, nine TCs were generated in the summer, i.e., two less than normal. The frequency of TC genesis in both June and July was equal to that of the climatology, but the number of TCs generated in August was two fewer than normal (Figure 1a). Four TCs made landfall over China in summer 2021, i.e., slightly fewer than normal; the frequency of TC landfall in June and July was close to the climatological value, but it was one fewer than normal in August (Figure 1b).

The region of TC genesis over the WNP was divided into three sub-regions, i.e., 110°E–120°E (SCS), 120°E–145°E (WNP1), and 145°E–180° to the dateline (WNP2), and the frequency of TC genesis in each sub-region was determined to analyze the specific features of these locations (Table 1). In 2018, the frequency of TC genesis in all three sub-regions was slightly higher than normal throughout the year. In the summer, the frequency of TC genesis was close to the climatological value over the SCS, but it was 43% and 122% higher than normal over WNP1 and WNP2, respectively. Thus, most TCs were generated over the eastern part of the TC genesis region of the WNP in summer 2018. In 2021, the frequency of TC genesis was equivalent to the climatological value for the entire year over the SCS and WNP1, but it was less than half of the climatological value over WNP2. In the summer, the frequency of TC genesis was close to the climatology over the SCS, but it was 37% and 26% lower than normal over WNP1 and WNP2, respectively. Thus, TCs were generated mainly in the western part of the TC genesis region of the WNP in summer 2021.

Table 1 Frequency of TC genesis over the three sub-regions in 2018 and 2021

Time	SCS (110°E–120°E)	WNP1 (120°E–145°E)	WNP2 (145°E–180°)
Summer of 2018	3	9	6
Summer of 2021	3	4	2
Summer climatology	2.3	6.3	2.7
All months in 2018	6	14	9
All months in 2021	5	14	3
Annual climatology	4.9	13.4	7.5

4. Environmental conditions in 2018 and 2021

In this section, we explore the possible causes for the differences in TC genesis over the WNP between the summers of 2018 and 2021 through a comparison of the large-scale environmental conditions and key circulation systems over the TC source region of the WNP.

4.1 Monsoon trough and environmental factors

Figure 2 shows the spatial distribution of the large-scale environmental factors and the monsoon trough that affected TC genesis over the WNP during the summers of 2018 and 2021. In summer 2018, the monsoon trough extended eastward to nearly 150°E, with positive relative vorticity anomalies in the monsoon trough region, and positive centers over the northern SCS and northeastern Philippines (Figure 2a). The tropical western Pacific region was dominated by westerly winds in the low-level wind field, and there were two anomalous cyclones over the northern SCS and northeastern Philippines (Figure 2c). In the convection field, there were extensive negative OLR anomalies over the TC genesis region, indicating active deep convection (Figure 2g). Additionally, there was strong upper-level divergence over the WNP (Figure 2c). Simultaneously, the vertical wind shear between the higher and lower troposphere over the northern SCS and northeastern Philippines was weak (Figure 2e). Thus, in summer 2018, the northern SCS and northeastern Philippines experienced enhanced convection, strong low-level tropospheric convergence, upper-level divergence, and weak vertical wind shear between the higher and lower troposphere. Such large-scale environmental conditions were conducive to TC genesis (Gong et al., 2022), leading to the unusually high frequency of TCs in summer 2018.

The environmental conditions in summer 2021 were almost the opposite of those in 2018. The monsoon trough extended only to around 135°E, and the TC genesis region was dominated by negative vorticity anomalies (Figure 2b). The WNP region was affected primarily by easterly winds, with an anomalous anticyclone over the SCS and eastern Philippines (Figure 2d). Except for the northeastern Philippines with negative OLR anomalies, most other parts of the WNP region were controlled by strong positive OLR anomalies (Figure 2h), indicating that deep convection was not active over most of the TC genesis region. The center of a positive divergence anomaly in the upper troposphere was located over the northeastern Philippines (Figure 2d). The vertical wind shear between the higher and lower troposphere over the TC genesis region was strong (Figure 2f). Thus, in summer 2021, most of the TC genesis region experienced suppressed convection, weak low-level convergence, and upper-level divergence concentrated only over the northeastern Philippines, together with strong vertical wind shear between the higher and lower troposphere. Consequently, the location of TC genesis was shifted further northwestward, and fewer TCs were generated.

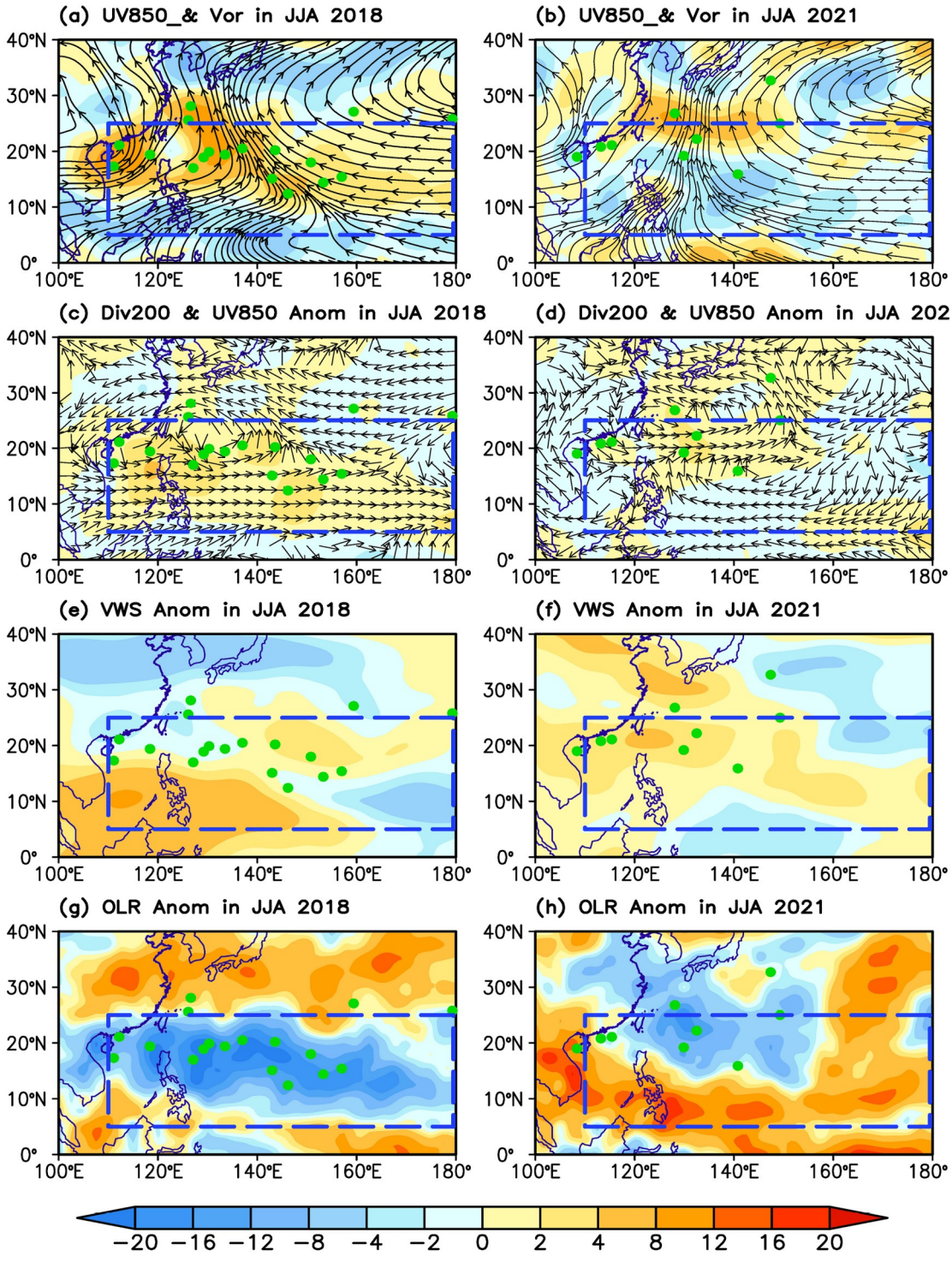

Figure 2 Distribution of the large-scale environmental factors in the summers of ((a), (c), (e), (g)) 2018 and ((b), (d), (f), (h)) 2021. (a), (b) 850-hPa horizontal wind stream field (bold blue lines indicate monsoon trough) and vorticity anomalies (shading, 10^{-5} s^{-1}). (c), (d) 850-hPa horizontal wind anomalies (vectors, m s^{-1}) and 200-hPa divergence anomalies (shading, 10^{-5} s^{-1}). (e), (f) Vertical wind shear between the 200- and 850-hPa levels (m s^{-1}). (g), (h) OLR anomalies (W m^{-2}). Green dots indicate locations of TC genesis, and blue dashed rectangle indicates the WNP TC genesis region (5°N–25°N, 110°E–180°).

4.2 WPSH and water vapor transport

The frequency and location of TC genesis in summer are closely related to the intensity and position of the WPSH (Gong et al., 2022). When the WPSH strengthens and extends westward, the frequency of TC genesis decreases, and vice versa. In summer 2018, the westernmost point of the WPSH was at approximately 140°E, further eastward than

normal, and the ridgeline of the WPSH was at 13.7°N, i.e., further northward than normal and at its northernmost position since 1951 (Figure 3a). Owing to the more northeastward location of the WPSH, the tropical southwest summer monsoon extended eastward and converged with the easterly winds on the southern flank of the WPSH, forming a center of strong water vapor convergence over the SCS and eastern Philippines region, which was conducive to TC genesis over the WNP (Figure 3a). However, in summer 2021, the WPSH was unusually strong and positioned further southwestward than normal. The WPSH-controlled regions were dominated by subsiding airflow, with poor moisture conditions and weak water vapor convergence (Figure 3b). The easterlies on the southern flank of the WPSH inhibited eastward extension of the summer monsoon, leading to a weak monsoon trough that was located further westward with conditions that were unfavorable for TC genesis.

5. SST and MJO anomalies in 2018 and 2021

One feature that was consistent in 2018 and 2021 was that the central and eastern equatorial Pacific experienced a La Niña event in the preceding winter (Figure 4). Specifically, from October 2017 to March 2018, the central and eastern equatorial Pacific experienced a La Niña event, which then decayed to a neutral state in spring 2018 (Figure 5a; Wang et al., 2018). Similarly, from August 2020 to March 2021, the central and eastern equatorial Pacific went through another La Niña event (Liu and Gao, 2021; Li et al., 2022, 2023), which transformed into a neutral state in spring 2021. Previous studies indicated that in summers with a higher frequency of TC genesis, the SSTs in the main TC genesis region of the WNP are anomalously warm during the previous winter and spring, whereas the central and eastern equatorial Pacific exhibits an extensive cold-tongue SSTA (Xiao et al., 2009). The large-scale low-level wind field of the preceding winter converges over the regions of warm SST, providing a background favorable for TC genesis in the subsequent summer. In spring, an abnormally active intertropical convergence zone in the equatorial Pacific advances toward the TC genesis region of the WNP, enhancing the positive feedback between the large-scale low-level moisture convergence and latent heat release in the atmosphere, which also favors TC genesis in the subsequent summer (Liu et al., 2021).

Given that the pattern of SSTA distribution in the central and eastern equatorial Pacific during the preceding winter and spring of both 2018 and 2021 was conducive to a higher frequency of TC genesis over the WNP in the subsequent summer, it is important to elucidate why the frequency of TC genesis differed markedly between the two years. In the following sections, we further compare and investigate the evolution characteristics and possible influences of the IOBM, PMM, and MJO, which have substantial impacts on the frequency of TC genesis over the WNP.

5.1 Indian Ocean Basin Mode

It is evident from Figure 5b that the positive IOBM turned negative in winter 2017/2018 and the negative phase persisted into the summer of 2018. This evolution of the tropical Indian Ocean SST turning into a cold anomaly aligns with the typical lagged response of La Niña decay (Ashok et al., 2003). However, the SSTA in the tropical Indian Ocean during 2020–2021 showed a different evolution (Figure 5b). After a temporary transition into the negative phase during winter 2020/2021, the IOBM index quickly became positive in March 2021, strengthened further in May, and then remained positive throughout the summer, which is a pattern that does not align with the lagged response of Indian Ocean SST in a year with La Niña decay.

To analyze the possible impact of the tropical Indian Ocean SSTA on the WPSH, the key circulation system affecting TC

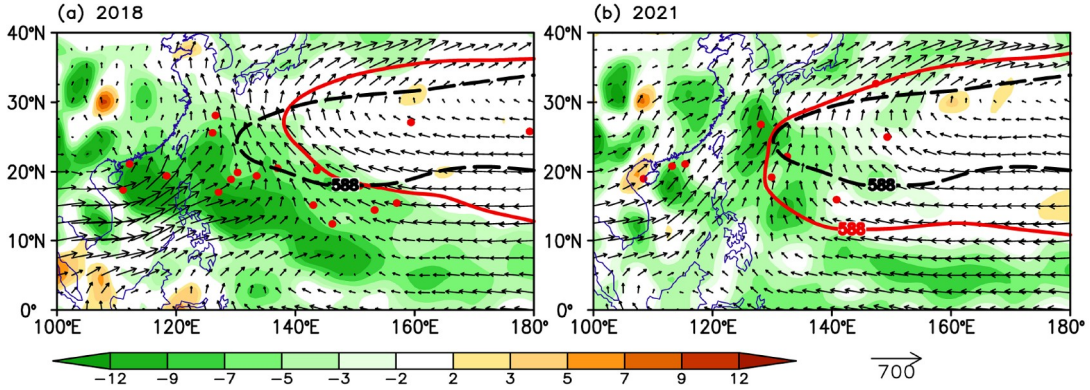

Figure 3 (a) Vertically integrated water vapor transport from the surface to 300 hPa (kg s^{-1} m^{-1}) and its divergence (10^{-5} kg s^{-1} m^{-2}) during the sumer of 2018. Red dots indicate the location of TCs genesis. Red solid and black dashed contours of 5880 gpm indicate the western Pacific subtropical high and the corresponding climatology, respectively. (b) Similar to (a) but of the summer of 2021.

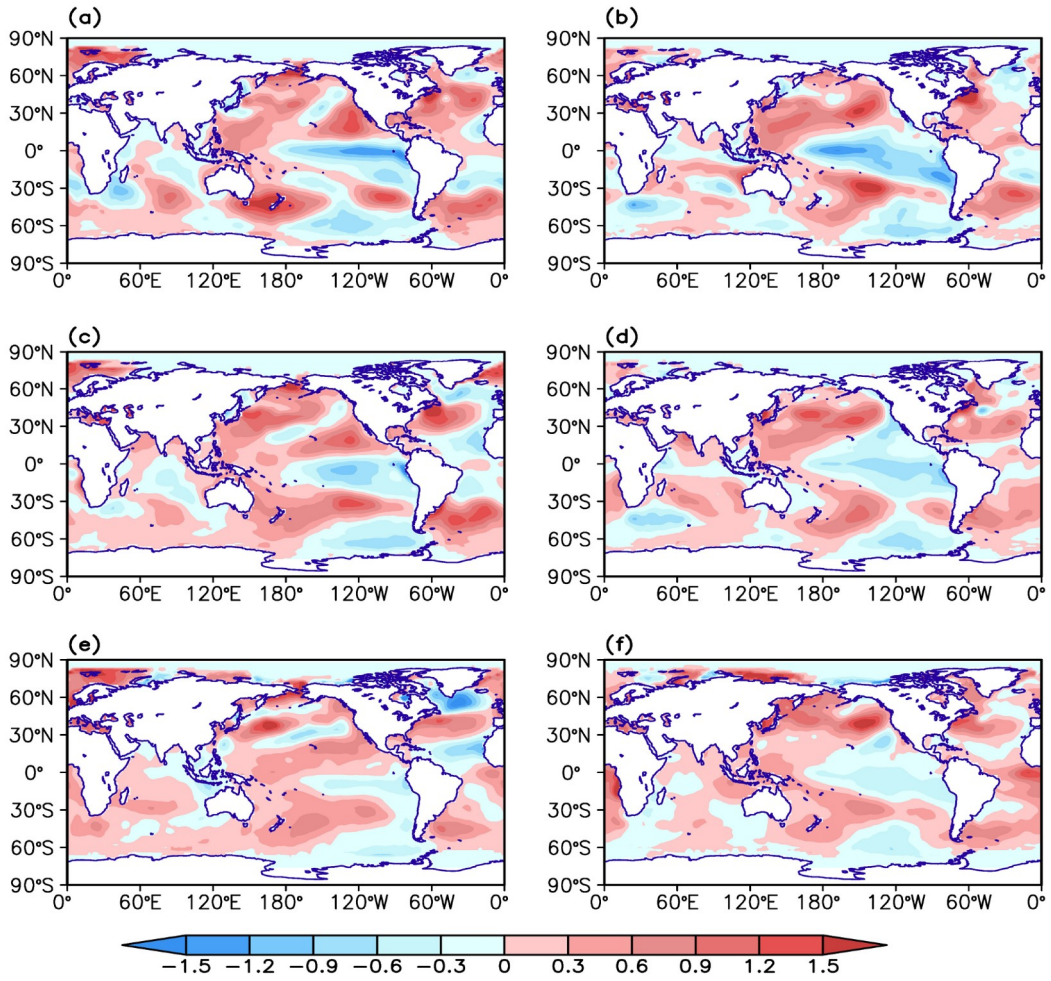

Figure 4 Evolution of seasonal SSTAs (°C): (a), (c), (e) from DJF 2017/2018, to MAM 2018, to JJA 2018, respectively, and (b), (d), (f) from DJF 2020/2021, to MAM 2021, to JJA 2021, respectively.

genesis, the correlation coefficients between the summer WPSH intensity and the IOBM indices from the preceding winter to the simultaneous summer were calculated after removal of the long-term linear trends (Figure 6). Moreover, the correlation coefficients with the Niño3.4 index were also calculated to compare the impacts of ENSO. The correlation coefficients between the summer WPSH intensity and the Niño3.4 indices in the preceding winter and spring are 0.57 and 0.51, respectively, both exceeding the 0.01 significance level. However, the correlation with the simultaneous summer is no longer significant, indicating that the summer WPSH is influenced mainly by SSTAs in the central and eastern equatorial Pacific during the preceding winter and spring. The relationship between the WPSH and the IOBM index is different from that of the Niño3.4 index. The correlation coefficients between the WPSH and the IOBM index in the preceding winter, spring, and the same summer are 0.51, 0.65, and 0.55, respectively, all exceeding the 0.01 significance level. It is implied that the influence of the tropical Indian Ocean SSTA on the WPSH can persist for longer than that of the Pacific SSTA, with more statistically significant impacts during spring and summer. The warm SSTA in the Indian Ocean can excite Kelvin waves through the Matsuno-Gill response, and form an anomalous anticyclone over the Bay of Bengal and the SCS, favoring the strengthening and westward extension of the WPSH (Matsuno, 1966; Gill, 1980; Liu and Chen, 2019; Ding et al., 2021; Liu and Gao, 2021).

Thus, the persistently warm SSTAs in the Indian Ocean during spring and summer 2021 were important factors in relation to the westward extension of the strengthened WPSH (Figure 3b). Such a situation inhibited eastward extension of the monsoon trough (Figure 2b) and suppressed tropical convection over the WNP (Figure 2h), creating conditions that were unfavorable for TC genesis and accounting for the low frequency of TC occurrence in summer 2021. In contrast, in 2018, the continuous cold SSTAs in the Indian Ocean during the winter, spring, and summer resulted in further northeastward displacement of the WPSH (Figure 3a), eastward extension of the monsoon trough (Figure 2a),

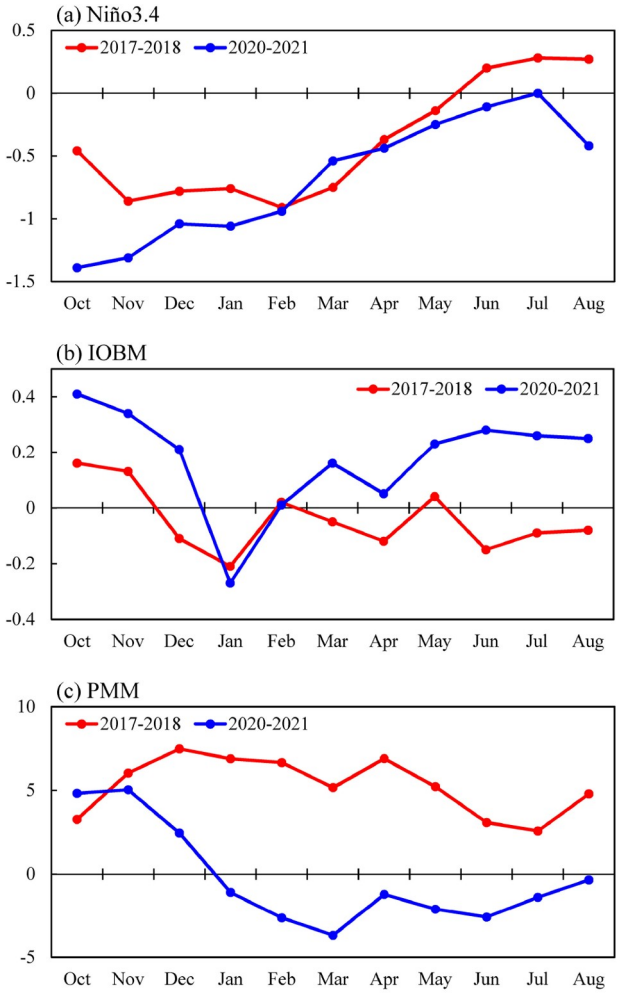

Figure 5 Time series of (a) Niño3.4, (b) IOBM, and (c) PMM indices from Oct 2017 to Aug 2018 (red lines), and from Oct 2020 to Aug 2021 (blue lines).

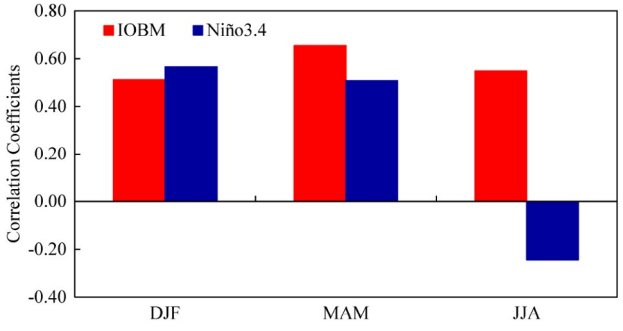

Figure 6 Correlation coefficients between the summer WPSH intensity index and the IOBM index (red bars) and the Niño3.4 index (blue bars) in DJF, MAM, and JJA during 1991–2020 (the long-term linear trends were removed from all the indices).

active tropical convection over the WNP (Figure 2g), low-level convergence, and upper-level divergence, which were conducive to TC genesis and accounted for the unusually high frequency of TC occurrence in 2018.

5.2 Pacific Meridional Mode

The PMM, defined by both SSTA and surface wind fields, reflects air-sea interaction. It is found that a statistically significant positive correlation exists between the PMM and TC activity in the WNP at the interannual timescale (Zhan et al., 2017). During the positive phase of the PMM, SSTAs in the subtropical northeastern Pacific are warmer than normal and extend into the western Pacific region, whereas the SSTAs in the tropical eastern Pacific are negative. Observation indicates that from winter 2017/2018 to summer 2018, the PMM index remained in a positive phase (Figure 5c), corresponding to warm SSTAs in the subtropical northeastern Pacific extending into the western Pacific, and cold SSTAs in the tropical eastern Pacific (Figure 4a, 4c, 4e). In the TC genesis region of the WNP, atmospheric heating via the Gill-Rossby wave response excited a low-level anomalous cyclone and an upper-level anomalous anticyclone, leading to weakened vertical wind shear and enhanced low-level relative vorticity (Figure 2a, 2c, 2f). This resulted in a weakened WPSH and a strengthened monsoon trough extending eastward, thereby promoting the generation and development of TCs over the WNP (Liu et al., 2019).

However, the positive phase of the PMM index during winter 2020/2021 turned to the negative phase in January 2021 and it remained in that state through into the summer. The negative phase of the PMM led to the strengthening of the WPSH and the formation of a low-level anomalous anticyclone over the TC genesis region of the WNP, which reduced relative vorticity and weakened the monsoon trough (Figure 2b, 2d, 2f), creating conditions unconducive to TC genesis. Thus, the divergent variation in the PMM was one of the influencing factors that caused the notable differences in TC genesis between the summers of 2018 and 2021.

5.3 Madden-Julian Oscillation

As an important mode of the tropical atmospheric circulation, the MJO activity with different phases corresponds to the distinct distributions of dynamic factors that trigger TC genesis over the WNP (Li and Zhou, 2012, 2013;Gong et al., 2022). When the MJO is in phases 2 and 3, the center of deep convection is to the west of the Maritime Continent (i.e., the equatorial eastern Indian Ocean region), corresponding to positive sea level pressure anomalies and suppressed convection over the WNP. Such environmental conditions are unfavorable for TC genesis. It is indicated that the frequency of TC genesis decreases substantially with the MJO in phases 2 and 3 (Liu et al., 2021). When the MJO is in phases 5 and 6, the center of deep convection moves to the WNP region. Correspondingly, the sea level pressure decreases in the western Pacific, the monsoon trough strengthens, and convective activity and low-level convergence increase, forming

large-scale dynamic environmental conditions suitable for TC genesis and development. Consequently, the frequency of TCs generated when the MJO is in phases 5 and 6 is more than double that when the MJO is in phases 2 and 3 (Pan et al., 2010).

Comparison of the MJO propagation activities in the summers of 2018 and 2021 reveals that the MJO stagnated in TC-favorable phases 5 and 6 for 55 days in summer 2018 (Figure 7a). This far exceeded the climatological value of 19.3 days, and it was the second longest period of stagnation since 1979, surpassed only by that in 1984 (61 days). There were 2 TCs generated during June 2–14 and 12 TCs generated between July 12 and August 18, when the MJO was in phases 5 and 6. Statistically, the TCs generated when the MJO was in phases 5 and 6 accounted for 77.8% of the total number TCs generated in the summer, indicating that the prolonged period of the MJO in phases 5 and 6 in summer 2018 contributed substantially to the observed TC activity.

In contrast, the MJO activity in summer 2021 was different. The MJO was in phases 5 and 6 for only 12 days, whereas it remained in TC-unfavorable phases 2 and 3 for as long as 47 days (Figure 7b), i.e., much longer than the climatological value of 26.6 days, making it the third longest period of such stagnation since 1979, surpassed only by 1995 (55 days) and 1983 (49 days). Therefore, the lower frequency of TC generation in summer 2021 was associated with the prolonged stagnation of the MJO in phases 2 and 3, when suppressed convection activity was dominant over the WNP. The difference in MJO activity between these two summers represents another external forcing factor responsible for the notable differences in the frequency of TC generation.

5.4 Contributions of external forcing

The above analysis indicates that tropical Indian Ocean SSTAs, the PMM, and prolonged stagnation of the MJO in different phases all had substantial impact on the frequency of TC genesis over the WNP in the summers of 2018 and 2021. To quantitatively assess the relative contributions of the IOBM, PMM, and MJO in different phases to the frequency of TC genesis in the two years, the regression coefficients for each of these influencing factors, which were first normalized, were calculated using linear regression to reconstruct the anomalies of TC genesis frequency for 2018 and 2021 (Table 2; Liu et al., 2023). Results show that the negative phase of the IOBM, positive phase of the PMM, and prolonged stagnation of the MJO in phases 5 and 6 all contributed positively to the higher frequency of TC genesis in 2018, with the greatest contribution from the MJO, followed by that of the IOBM, and the smallest contribution from the PMM. In 2021, the positive phase of the IOBM, negative phase of the PMM, and prolonged stagnation of the MJO in phases 2 and 3 collectively led to the lower frequency of TC genesis, with the IOBM and MJO contributing equally and the PMM contributing less. Hence, despite the similar La Niña background, the differences in the frequency of TC genesis over the WNP between the summer of 2018 and 2021 were jointly influenced by tropical Indian Ocean SSTAs, the PMM, and MJO activity anomalies, with the contributions from the tropical Indian Ocean SSTAs and MJO activity anomalies being more important than those from the PMM.

6. Summary and discussion

Both 2018 and 2021 were years with La Niña decay, but there were notable differences in TC activity over the WNP between the summers of these two years. In summer 2018, 18 TCs were generated, mainly over central and eastern parts of the WNP, of which 8 made landfall on the coast of China; both the frequency of genesis and the number of landfalling TCs were statistically significantly higher than the climatological values. In contrast, only 9 TCs were generated in summer 2021, primarily concentrated in the western WNP and the SCS regions, of which 4 made landfall on the coast of China. Thus, the frequency of TC genesis and the number of landfalling TCs were markedly lower in 2021 than in 2018. This work investigated the large-scale environmental conditions, tropical ocean thermal conditions, and low-fre-

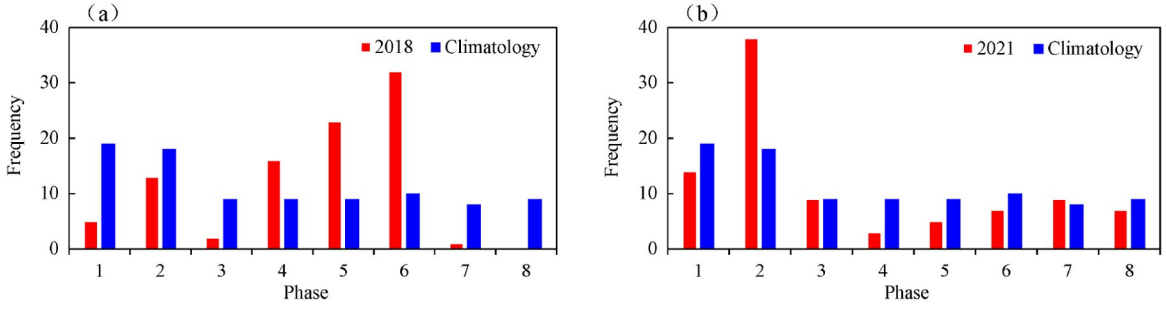

Figure 7 Frequencies of the MJO at phases 1–8 (red bars) in the summers of (a) 2018 and (b) 2021. Blue bars indicate the climatological frequencies for individual MJO phases. Units: days.

Table 2 Reconstruction of the frequency anomalies of WNP TC genesis based on the normalized IOBM, PMM, and MJO indices[a)]

External forcing	Regression coefficients	2018	2021
IOBM	−2.89**	2.98	−1.88
PMM	1.14*	1.22	−0.4
MJO_{56}	1.98**	3.65	0.29
MJO_{23}	−1.70**	−0.62	−1.86

a) * reaching the 0.05 significance level; ** reaching the 0.01 significance level

quency oscillation activities during these two years to reveal their possible impacts on the differences in TC activity over the WNP under a similar background of La Niña decay.

In 2017–2018, the tropical Indian Ocean SST showed the typical response to a Pacific La Niña event, turning to a cold anomaly in winter that persisted into the summer of 2018. Consequently, the WPSH shifted further northeastward in the summer, the monsoon trough extended eastward to nearly 150°E, convection was active over most of the WNP TC genesis region, with anomalous low-level convergence and upper-level divergence, and weak vertical wind shear between the high and low troposphere, which represent conditions conducive to TC genesis. This led to the notably higher frequency of TC genesis in summer 2018.

In contrast, the SST evolution in the tropical Indian Ocean during 2020–2021 did not exhibit the typical response to a La Niña event. After a temporary shift to a cold anomaly in January 2021, it quickly turned to a positive anomaly in March 2021 and it remained positive into the summer. The persistent warming of the tropical Indian Ocean caused the WPSH to be strong and extend further westward in the summer, and the monsoon trough extended eastward to only around 135°E. Convection was suppressed over most of the TC genesis region, with weak low-level convergence and large vertical wind shear. The region of strong upper-level divergence was confined to the northeastern Philippines. Consequently, the frequency of TC genesis was much lower than normal, and the region of TC genesis was displaced further northwestward.

Additionally, the PMM index remained in a positive phase from winter 2017/2018 through to summer 2018, which excited a low-level anomalous cyclone and an upper-level anomalous anticyclone over the TC genesis region of the WNP via the Gill-Rossby wave response. This led to weakened vertical wind shear and enhanced low-level relative vorticity, promoting TC genesis and development. However, in 2021, the PMM index turned to a negative phase in January and it remained in that state through the summer, forming an anomalous anticyclone in the lower troposphere over the TC genesis region, reducing relative vorticity, and weakening the monsoon trough, which represented conditions unconducive to TC genesis over the WNP.

Evident differences in MJO activity also existed between the summers of 2018 and 2021. In summer 2018, the MJO stagnated in phases 5 and 6 for a prolonged period, strengthening convection and convergence over the western Pacific, creating favorable large-scale dynamic conditions for TC genesis and development. In contrast, the MJO was mostly in TC-unfavorable phases 2 and 3 during summer 2021, stagnating for 47 days. During this period, the center of convection was confined to the western Maritime Continent, while convection activities were suppressed over most of the WNP region, which was unconducive to TC genesis.

Thus, despite the similar La Niña background, notable differences in tropical Indian Ocean SSTAs, the PMM, and MJO activity led to the observed differences in the frequency of TC genesis over the WNP between the summers of 2018 and 2021. Quantitative assessments of the contributions of these influencing factors indicated that tropical Indian Ocean SSTA and MJO activity anomalies had greater impact than the PMM. These findings provide a more reliable reference for predicting TC activity over the WNP.

In addition to the impacts of ENSO, tropical Indian Ocean SSTAs, the PMM, and MJO activity analyzed in this work, other studies have suggested that the thermal state of the Western Pacific Warm Pool (Chen and Huang, 2008), tropical North Atlantic SSTA (Yu et al., 2016), spring SSTA to the east of Australia (Zhou and Cui, 2010), and winter-spring sea ice extent in the North Pacific (Fan, 2007) can also influence the genesis and development of TCs over the WNP. Further comparative analyses of analog years and the use of the Genesis Potential Index could be employed to quantitatively diagnose all the external forcing and corresponding physical processes that affect TC genesis (Gong et al., 2022). Moreover, the factors and physical mechanisms that affect the path and landfalling of TCs are also worthy of further research. These issues will be explored in our future work to enhance the capability for prediction of WNP TC activity.

Acknowledgements *This work was supported by the National Key R&D Program of China (Grant No. 2022YFF0801604), the National Natural Science Foundation of China (Grant No. 42175056), the Provincial Natural Science Foundation of Anhui (Grant No. 2208085UQ10), the Civilian Space Programme of China (Grant No. Do40305), the Fengyun Application Pioneering Project (Grant No. FY-APP-ZX-2023.02), the China Meteorological Administration Innovation and Development Project (Grant No. CXFZ2024J048), and the China Meteorological Administration Youth Innovation Team (Grant No. CMA2024QN06).*

Conflict of interest The authors declare that they have no conflict of interest.

References

Alexander M A, Bladé I, Newman M, Lanzante J R, Lau N C, Scott J D. 2002. The atmospheric bridge: The influence of ENSO teleconnections

on air-sea interaction over the global oceans. J Clim, 15: 2205–2231
Ashok K, Behera S K, Rao S A, Weng H, Yamagata T. 2007. El Niño Modoki and its possible teleconnection. J Geophys Res, 112: 2006JC003798
Ashok K, Guan Z, Yamagata T. 2003. A look at the relationship between the ENSO and the Indian Ocean dipole. J Meteorol Soc Jpn, 81: 41–56
Briegel L M, Frank W M. 1997. Large-scale influences on tropical cyclogenesis in the Western North Pacific. Mon Weather Rev, 125: 1397–1413
Camargo S J, Emanuel K A, Sobel A H. 2007. Use of a genesis potential index to diagnose ENSO effects on tropical cyclone genesis. J Clim, 20: 4819–4834
Chambers D P, Tapley B D, Stewart R H. 1999. Anomalous warming in the Indian Ocean coincident with El Niño. J Geophys Res, 104: 3035–3047
Chan J C L. 1985. Tropical cyclone activity in the Northwest Pacific in relation to the El Niño/Southern Oscillation phenomenon. Mon Weather Rev, 113: 599–606
Chan J C L. 2000. Tropical cyclone activity over the Western North Pacific associated with El Niño and La Niña events. J Clim, 13: 2960–2972
Chen G, Huang R. 2006. Research on climatological problems of tropical cyclone and T-yphoon activity in western North Pacific (in Chinese). Adv Earth Sci, 21: 610–616
Chen G, Huang R. 2008. Influence of monsoon over the warm pool on interannual variation on tropical cyclone activity over the western North Pacific. Adv Atmos Sci, 25: 319–328
Chen G, Huang R. 2009. Dynamical effects of low frequency oscillation on tropical cyclogenesis over the Western North Pacific and the physical mechanisms (in Chinese). Chin J Atmos Sci, 33: 205–214
Chen G, Tam C. 2010. Different impacts of two kinds of Pacific Ocean warming on tropical cyclone frequency over the western North Pacific. Geophys Res Lett, 37: 2009GL041708
Chen L, Gong Z, Wu J, Li W. 2019. Extremely active tropical cyclone activities over the Western North Pacific and South China Sea in summer 2018: Joint effects of decaying La Niña and intraseasonal oscillation. J Meteorol Res, 33: 609–626
Chia H H, Ropelewski C F. 2002. The interannual variability in the genesis location of tropical cyclones in the Northwest Pacific. J Clim, 15: 2934–2944
Chiang J C H, Vimont D J. 2004. Analogous Pacific and Atlantic meridional modes of tropical atmosphere-ocean variability. J Clim, 17: 4143–4158
Ding Y, Liu Y, Hu Z Z. 2021. The record-breaking Mei-yu in 2020 and associated atmospheric circulation and tropical SST anomalies. Adv Atmos Sci, 38: 1980–1993
Du X G, Yu J H. 2020. Contribution of environmental factors to the change of tropical cyclone frequency in tne summer of ENSO developing and decaying years (in Chinese). J Trop Meteorol, 36: 244–253
Du Y, Yang L, Xie S P. 2011. Tropical Indian Ocean influence on Northwest Pacific tropical cyclones in summer following strong El Niño. J Clim, 24: 315–322
Fan K. 2007. North Pacific sea ice cover, a predictor for the Western North Pacific typhoon frequency? Sci China Ser D-Earth Sci, 50: 1251–1257
Gao S, Zhu L, Zhang W, Chen Z. 2018. Strong modulation of the Pacific meridional mode on the occurrence of intense tropical cyclones over the Western North Pacific. J Clim, 31: 7739–7749
Gill A E. 1980. Some simple solutions for heat-induced tropical circulation. Q J R Meteorol Soc, 106: 447–462
Gong Z, Liu Y, Hu Z Z, Liang P. 2022. Tropical cyclone activities over the western north Pacific in summer 2020: Transition from silence in July to unusually active in August. Front Earth Sci, 10: 843990
Han R, Wang H, Hu Z Z, Kumar A, Li W, Long L N, Schemm J K E, Peng P, Wang W, Si D, Jia X, Zhao M, Vecchi G A, LaRow T E, Lim Y K, Schubert S D, Camargo S J, Henderson N, Jonas J A, Walsh K J E. 2016. An assessment of multimodel simulations for the variability of western north Pacific tropical cyclones and its association with ENSO. J Clim, 29: 6401–6423
Ho C H, Baik J J, Kim J H, Gong D Y, Sui C H. 2004. Interdecadal changes in summertime typhoon tracks. J Clim, 17: 1767–1776
Hong C C, Lee M Y, Hsu H H, Tseng W L. 2018. Distinct influences of the ENSO-like and PMM-like SST anomalies on the mean TC genesis location in the Western North Pacific: The 2015 summer as an extreme example. J Clim, 31: 3049–3059
Hu J, Wang Y Q. 1992. Atmosphere and ocean low-frequency oscillation and their effects on tropical cyclone track over the Northwestern Pacific (in Chinese). Acat Meteorol Sin, 50: 420–428
Huang B, Liu C, Banzon V, Freeman E, Graham G, Hankins B, Smith T, Zhang H M. 2021. Improvements of the daily optimum interpolation sea surface temperature (DOISST) version 2.1. J Clim, 34: 2923–2939
Huangfu J, Chen W, Huang R, Feng J. 2019. Modulation of the impacts of the Indian Ocean Basin Mode on tropical cyclones over the Northwest Pacific during the boreal summer by La Niña Modoki. J Clim, 32: 3313–3326
Huangfu J, Huang R, Chen W, Feng T. 2018. Causes of the active typhoon season in 2016 following a strong El Niño with a comparison to 1998. Intl J Clim, 38: e1107
Huang R, Chen G. 2007. Besearch on interannual variations of tracks tropical cyclones over Northwest pacific and their physical mechanism (in Chinese). Acta Meteorol Sin, 65: 683–694
Huang Y, Li C, Wang Y. 2009. The Pacific meridional mode of coupled ocean-atmosphere and the connection with frequeccy of tropical cyclones activity over the western North Pacific (in Chinese). J Trop Meteorol, 25: 169–174
Huo L, Guo P, Hameed S N, Jin D. 2015. The role of tropical Atlantic SST anomalies in modulating western North Pacific tropical cyclone genesis. Geophys Res Lett, 42: 2378–2384
Huo L, Guo P, Zhang F. 2016. Impact of summer tropical Atlantic SST anomaly on western North Pacific tropical cyclone genesis (in Chinese). Trans Atmos Sci, 39: 55–63
Kalnay E, Kanamitsu M, Kistler R, Collins W, Deaven D, Gandin L, Iredell M, Saha S, White G, Woollen J, Zhu Y, Leetmaa A, Reynolds R, Chelliah M, Ebisuzaki W, Higgins W, Janowiak J, Mo K C, Ropelewski C, Wang J, Jenne R, Joseph D. 1996. The NCEP/NCAR 40-year reanalysis project. Bull Amer Meteorol Soc, 77: 437–471
Kao H Y, Yu J Y. 2009. Contrasting eastern-Pacific and central-Pacific types of ENSO. J Clim, 22: 615–632
Kim H M, Webster P J, Curry J A. 2011. Modulation of North Pacific Tropical cyclone activity by three phases of ENSO. J Clim, 24: 1839–1849
Kug J S, Jin F F, An S I. 2009. Two types of El Niño events: Cold tongue El Niño and warm pool El Niño. J Clim, 22: 1499–1515
Li R C Y, Zhou W. 2012. Changes in Western Pacific tropical cyclones associated with the El Niño-Southern Oscillation cycle. J Clim, 25: 5864–5878
Li R C Y, Zhou W. 2013. Modulation of western North Pacific tropical cyclone activity by the ISO. Part I: Genesis and intensity. J Clim, 26: 2904–2918
Li X, Hu Z, Tseng Y, Liu Y, Liang P. 2022. A historical perspective of the La Niña event in 2020/2021. J Geophys Res-Atmos, 127: e2021JD035546
Li X, Hu Z, McPhaden M J, Zhu C, Liu Y. 2023. Triple-dip La Niñas in 1998–2001 and 2020–2023: Impact of mean state changes. J Geophys Res-Atmos, 128: e2023JD038843
Liang P, Hu Z Z, Ding Y, Qian Q. 2021. The extreme Mei-yu season in 2020: Role of the madden-julian oscillation and the cooperative influence of the Pacific and Indian Oceans. Adv Atmos Sci, 38: 2040–2054
Liu C, Zhang W, Stuecker M F, Jin F. 2019. Pacific meridional mode-Western North Pacific Tropical cyclone linkage explained by tropical Pacific quasi-decadal variability. Geophys Res Lett, 46: 13346–13354
Liu C, Zhang W, Jiang F, Stuecker M F, Huang Z. 2021. Record-low WNP tropical cyclone activity in early summer 2020 due to Indian Ocean warming and Madden-Julian oscillation activity. Geophys Res Lett, 48: e2021GL094578
Liu Y, Chen L. 2019. Features and possible causes for the spring climate anomalies in 2019 (in Chinese). Meteorol Mon, 45: 1483–1493

Liu Y, Hu Z, Wu R. 2020. Was the extremely wet winter of 2018/2019 in the lower reach of the Yangtze River driven by El Niño-Southern Oscillation? Intl J Clim, 40: 6441–6457
Liu Y, Gao H. 2021. Features and possible causes of climate anomalies in China in spring 2021 (in Chinese). Meteorol Mon, 47: 1277–1288
Liu Y, Li D, Hu Z Z, Wu R, Wu J, Ding Y. 2023. The extremely wet spring of 2022 in Southwest China was driven by La Niña and Tibetan Plateau warming. Atmos Res, 289: 106758
Madden R A, Julian P R. 1971. Detection of a 40–50 day oscillation in the zonal wind in the tropical Pacific. J Atmos Sci, 28: 702–708
Matsuno T. 1966. Quasi-geostrophic motions in the Equatorial area. J Meteorol Soc Jpn, 44: 25–43
Pan J, Li C, Song J. 2010. The modulation of Madden-Julian Oscillation on typhoons in the northwestern Pacific Ocean (in Chinese). Chin J Atmos Sci, 34: 1059–1070
Qian D L, Guan Z Y. 2019. Impacts of tropical Indian Ocean sea surface temperature anomalies on the variation of western Pacific subtropical high in the summer: Dependent and independent of ENSO (in Chinese). Acta Meteorol Sin, 77: 442–455
Ren H L, Jin F F. 2011. Niño indices for two types of ENSO. Geophys Res Lett, 38: L04704
Ritchie E A, Holland G J. 1999. Large-scale patterns associated with tropical cyclogenesis in the Western Pacific. Mon Weather Rev, 127: 2027–2043
Sobel A H, Maloney E D. 2000. Effect of ENSO and the MJO on western North Pacific tropical cyclones. Geophys Res Lett, 27: 1739–1742
Stuecker M F, Timmermann A, Jin F F, McGregor S, Ren H L. 2013. A combination mode of the annual cycle and the El Niño/Southern Oscillation. Nat Geosci, 6: 540–544
Tao L, Cheng S C. 2012. Impact of Indian Ocean Basin warming and ENSO on tropical cyclone activities over the Western Pacific (in Chinese). Chin J Atmos Sci, 6: 1223–1235
Wang B, Chan J C L. 2002. How strong ENSO events affect tropical storm activity over the Western North Pacific. J Clim, 15: 1643–1658
Wang C, Wang B, Wu L. 2018. Abrupt breakdown of the predictability of early season typhoon frequency at the beginning of the twenty-first century. Clim Dyn, 52: 3809–3822
Wang Z, Liu Y, Ding T, Li D, Hong J L. 2018. Features and Possible Causes for the Climate Anomalies in spring 2018(in Chinese). Meteorol Mon, 44: 1360–1369
Wheeler M C, Hendon H H. 2004. An all-season real-time multivariate MJO Index: Development of an index for monitoring and prediction. Mon Weather Rev, 132: 1917–1932
Wu Y, Hong C, Chen C. 2018. Distinct effects of the two strong El Niño events in 2015–2016 and 1997–1998 on the Western North Pacific monsoon and tropical cyclone activity: Role of subtropical Eastern North Pacific warm SSTA. J Geophys Res-Oceans, 123: 3603–3618
Xiao F, Xiao Z. 2010. Characteristics of tropical cyclones in China and their impacts analysis. Nat Hazards, 54: 827–837
Xiao Z, Liang H, Li C. 2009. The relationship between the summer typhoon genesis over the western North Pacific and South China Sea and the main climatic conditions in the preceding winter to spring. Acta Meteorol Sin, 67: 90–99
Xie S P, Hu K, Hafner J, Tokinaga H, Du Y, Huang G, Sampe T. 2009. Indian Ocean capacitor effect on Indo3Western Pacific climate during the summer following El Niño. J Clim, 22: 730–747
Ying M, Zhang W, Yu H, Lu X, Feng J, Fan Y, Zhu Y, Chen D. 2014. An overview of the China meteorological administration tropical cyclone database. J Atmos Ocean Tech, 31: 287–301
Yu J, Li T, Tan Z, Zhu Z. 2016. Effects of tropical North Atlantic SST on tropical cyclone genesis in the western North Pacific. Clim Dyn, 46: 865–877
Zhan R, Wang Y, Lei X. 2011. Contributions of ENSO and East Indian Ocean SSTA to the interannual variability of Northwest Pacific tropical cyclone frequency. J Clim, 24: 509–521
Zhan R, Wang Y, Wen M. 2013. The SST gradient between the Southwestern Pacific and the Western Pacific Warm Pool: A new factor controlling the Northwestern Pacific tropical cyclone genesis frequency. J Clim, 26: 2408–2415
Zhan R, Wang Y, Liu Q. 2017. Salient differences in tropical cyclone activity over the Western North Pacific between 1998 and 2016. J Clim, 30: 9979–9997
Zhang J Y, Wu L G, Zhang Q.2011. Tropical cyclone damages in China under the background of global warming (in Chinese). J Trop Meteorol, 27: 442–454
Zhang W, Huang Z, Jiang F, Stuecker M F, Chen G, Jin F. 2020. Exceptionally persistent Madden-Julian Oscillation activity contributes to the extreme 2020 East Asian summer monsoon rainfall. Geophys Res Lett, 48: e2020GL091588
Zhang W, Li H, Jin F F, Stuecker M F, Turner A G, Klingaman N P. 2015. The annual-cycle modulation of meridional asymmetry in ENSO's atmospheric response and its dependence on ENSO zonal structure. J Clim, 28: 5795–5812
Zhang W, Vecchi G A, Murakami H, Villarini G, Jia L. 2016. The Pacific Meridional Mode and the occurrence of tropical cyclones in the Western North Pacific. J Clim, 29: 381–398
Zhang W, Vecchi G A, Villarini G, Murakami H, Rosati A, Yang X, Jia L, Zeng F. 2017a. Modulation of western North Pacific tropical cyclone activity by the Atlantic Meridional Mode. Clim Dyn, 48: 631–647
Zhang W, Vecchi G A, Villarini G, Murakami H, Gudgel R, Yang X. 2017b. Statistical-dynamical seasonal forecast of Western North Pacific and East Asia landfalling tropical cyclones using the GFDL FLOR coupled climate model. J Clim, 30: 2209–2232
Zhou B, Cui X. 2010. Sea surface temperature east of Australia: A predictor of tropical cyclone frequency over the western North Pacific (in Chinese)? Chin Sci Bull, 55: 3053–3059

(Editorial handling: Bangqi XU)